Inorg. Chem. **2007**, *46*, 2132–2138

$Ln_{14}Na_3Ru_6O_{36}$ (Ln = Pr, Nd): Two New Complex Lanthanide-Containing Oxides of Ruthenium

William R. Gemmill, Mark D. Smith, and Hans-Conrad zur Loye*

Department of Chemistry and Biochemistry, University of South Carolina, Columbia, South Carolina 29208

Received September 8, 2006

The lanthanide-containing ruthenium oxides $Ln_{14}Na_3Ru_6O_{36}$ (Ln = Pr, Nd) were prepared as single crystals from molten sodium hydroxide. The two compounds crystallize in the rhombohedral space group $R\bar{3}c$ with cell constants of a = 9.7380(2) and 9.6781(2) Å and c = 55.5716(18) and 55.4156(18) Å for $Ln_{14}Na_3Ru_6O_{36}$ (Ln = Pr, Nd), respectively. The structure of the two compounds is composed of two types of slabs that alternate in an AB fashion. Each slab consists of three layers and are arranged to yield a unit cell with a 12-layer structure. Both compounds exhibit magnetic behavior consistent with canted antiferromagnetism.

Introduction

In recent years, many complex oxides of ruthenium have been reported, both with commonly observed and with unusual structure types. Examples include the double perovskites Ln_2NaRuO_6 (Ln = La, Pr, Nd)[1] and La_2LiRuO_6,[2] the metallic perovskite $CaCu_3Ga_2Ru_2O_{12}$,[3] the 6*H*-perovskite $Ba_3NaRu_2O_9$,[4] the more complex 10*H*-perovskite $Ba_5Na_2Ru_3O_{14}$,[5] and the lanthanum-containing ruthenate $La_7Ru_3O_{18}$.[6] These compounds have been prepared by various methods, including standard solid-state reaction, high-pressure synthesis, electrosynthesis from molten hydroxide, and crystallization from molten hydroxide solutions.

Generally, the synthesis of new oxides is achieved by the identification of known phases followed by the subsequent postulation of phases that have the potential to exist. Such postulations rely, at least in part, on chemical composition, where considerations include the coordination preference, oxidation state, and thermodynamic stability of the desired combination of constituent elements. While this method has led to the preparation of an enormous number of complex oxides, it relies on a starting point in the form of a known structure or known composition. In this respect, crystal growth from high-temperature solutions can help, as it is an effective technique to prepare compounds whose potential existence was not previously conceived by any deductive reasoning. This is particularly applicable for the case of complex oxides, where it can be argued that structural complexity increases concomitantly with the incorporation of more species into the final product. A classic example involves the elemental substitution in simple perovskites, ABO_3, where half of the B cations are replaced by B′ cations, yielding the composition $A_2BB'O_6$ and effectively doubling the unit cell while enabling additional structural variability with respect to the arrangement of the BO_6 and $B'O_6$ octahedra.[7]

Our group has focused on materials discovery by crystal growth, where molten hydroxides are used as a solvent for the crystallization of new complex oxides, including ruthenium oxides containing lanthanide metals. This well-established method is superbly suited for oxide crystal growth, and there exist a multitude of published compositions containing elements from nearly every section of the periodic table.[8] In addition, crystal growth from solution has advantages over standard ceramic methods, such as enhanced mixing of reagents, which eliminates the typical diffusion limitations, the possibility of controlling the nature of the species in solution (i.e., oxidation state), and most impor-

* To whom correspondence should be addressed. E-mail: zurloye@mail.chem.sc.edu.

(1) Gemmill, W. R.; Smith, M. D.; zur Loye, H.-C. *J. Solid State Chem.* **2004**, *177*, 3560.
(2) Battle, P. D.; Grey, C. P.; Hervieu, M.; Martin, C.; Moore, C. A.; Paik, Y. *J. Solid State Chem.* **2003**, *175*, 20.
(3) Byeon, S.-H.; Lee, S.-S.; Parise, J. B.; Woodward, P. M.; Hur, N. H. *Chem. Mater.* **2004**, *16*, 3697.
(4) Stitzer, K. E.; Smith, M. D.; Gemmill, W. R.; zur Loye, H.-C. *J. Am. Chem. Soc.* **2002**, *124*, 13877.
(5) Quarez, E.; Mentre, O. *Solid State Sci.* **2003**, *5*, 1105.
(6) Khalifah, P.; Huang, Q.; Ho, D. M.; Zandbergen, H. W.; Cava, R. J. *J. Solid State Chem.* **2000**, *155*, 189.
(7) Mitchell, R. M. *Perovskites: Modern and Ancient*; Almaz Press: Thunder Bay, Canada, 2002.
(8) Elwell, D.; Scheel, H. J. *Crystal Growth from High-Temperature Solutions*; Academic Press: New York, 1975.

10.1021/ic0617083 CCC: $37.00
Published on Web 02/27/2007

tantly, the ability to employ single-crystal X-ray diffraction for accurate structure determination of complex materials. Many high-temperature solutions have been utilized in the crystal growth of oxide materials, including alkali and alkaline earth carbonates, halides, peroxides, superoxides, and hydroxides.[9−14]

We have developed an effective route for synthesizing single crystals of new complex oxides using sealed silver tubes to help maintain the proper reaction conditions for the dissolution of all reagents, a prerequisite for crystal growth.[1,15] From a series of investigations of this type, two new ruthenates, $Ln_{14}Na_3Ru_6O_{36}$ (Ln = Pr, Nd), have been isolated as single crystals from molten sodium hydroxide in sealed silver tubes. Herein, we report on the synthesis, crystal structures, and magnetic properties of $Pr_{14}Na_3Ru_6O_{36}$ and $Nd_{14}Na_3Ru_6O_{36}$.

Experimental Section

A. Crystal Growth. For $Nd_{14}Na_3Ru_6O_{36}$, 1 mmol of RuO_2 (synthesized by heating Ru powder (Engelhard, 99.5%) in air for 24 h), 0.9 mmol of Nd_2O_3 (activated by heating the oxide from the bottle (Alfa, 99.9%) in air at 1000 °C for 12 h), and 6.0 g of NaOH (Fisher, reagent grade) were added to a 0.5 in. diameter silver tube that had been flame sealed at one end and securely crimped shut on the other end. The reaction mixture was heated at a rate of 10 °C/min to 600 °C, held at temperature for 12 h, and then quickly cooled to room temperature by turning off the furnace.

For $Pr_{14}Na_3Ru_6O_{36}$, 0.5 mmol of RuO_2, 0.5 mmol of Os metal (J & J Materials, Inc., 99.98%), 1 mmol of Pr_2O_3 (prepared by heating $Pr(OH)_3$ in a 5/95% H_2/N_2 atmosphere at 1000 °C for 24 h), and 4.5 g of NaOH were added to a silver tube. The reaction mixture was heated at a rate of 10 °C/min to 600 °C, held at temperature for 12 h, and then cooled to 500 °C at 1 °C/min followed by shutting off the furnace.

In both cases, the crystals were removed from the flux by washing with water, aided by the use of sonication.

Initial crystal growth experiments were aimed at the preparation of a mixed osmium−ruthenium oxide which, however, led to the growth of the ruthenates $Nd_{14}Na_3Ru_6O_{36}$ and $Pr_{14}Na_3Ru_6O_{36}$ instead. In the case of $Nd_{14}Na_3Ru_6O_{36}$, the synthesis was readily repeated in the absence of osmium in the reaction mixture. In the case of $Pr_{14}Na_3Ru_6O_{36}$, however, crystals were obtained only in the presence of osmium metal in the reaction mixture. Reactions carried out in the absence of osmium powder did not lead to the formation of $Pr_{14}Na_3Ru_6O_{36}$ and, in fact, yielded single crystals of Pr_2NaRuO_6.[1]

Experience has shown that hydroxide flux reactions aimed at the incorporation of praseodymium require Pr_2O_3 and not Pr_6O_{11} as a starting material. Hence, treatment of $Pr(OH)_3$ in a 5/95% H_2/N_2 atmosphere to yield Pr_2O_3 is typically necessary for the successful incorporation of praseodymium into oxide crystals by the hydroxide flux route. We believe that a possible role for the osmium in the reaction mixture is to act as a sacrificial reductant that keeps praseodymium in the +3 oxidation state long enough for crystal growth of $Pr_{14}Na_3Ru_6O_{36}$ to occur. As neodymium does not have a stable +4 oxidation state, osmium is not necessary for the synthesis of $Nd_{14}Na_3Ru_6O_{36}$.

B. Single-Crystal X-ray Diffraction. X-ray intensity data from a black hexagonal block and a small black chip were measured at 293 and 294 K for $Nd_{14}Na_3Ru_6O_{36}$ and $Pr_{14}Na_3Ru_6O_{36}$, respectively, on a Bruker SMART APEX CCD-based diffractometer (Mo Kα radiation, $\lambda = 0.71073$ Å).[16] For $Nd_{14}Na_3Ru_6O_{36}$, the data collection covered reciprocal space to $2\theta_{max} = 65.7°$, with an average redundancy to $2\theta_{max}$ of 8.1 and $R_{int} = 0.0394$, and for $Pr_{14}Na_3Ru_6O_{36}$, the data collection covered reciprocal space to $2\theta_{max} = 65.1°$, with an average redundancy to $2\theta_{max}$ of 9.3 and $R_{int} = 0.0751$. Raw data frame integration and Lp corrections were performed with SAINT+.[16] Final unit cell parameters were determined by least-squares refinement of 5636 ($Nd_{14}Na_3Ru_6O_{36}$) and 6848 ($Pr_{14}Na_3Ru_6O_{36}$) reflections from the data sets with $I > 5\sigma I$. Analysis of the data showed negligible crystal decay during data collection. The data were corrected for absorption effects with SADABS.[16] Full-matrix least-squares refinement against F^2 were performed with SHELXTL.[17]

For $Nd_{14}Na_3Ru_6O_{36}$, systematic absences indicated the space groups $R3c$ and $R\bar{3}c$, the latter of which was confirmed. Metal atom positions were located by direct methods and assigned as Nd, Ru, or Na by coordination environment and displacement parameter behavior. Oxygen atoms were located in difference maps. The structure contains three inequivalent Nd positions, three inequivalent Ru positions, two inequivalent Na positions, and six independent oxygen atoms. After location and correct scattering factor assignment, full anisotropic refinement resulted in reasonable displacement parameters for all atoms. Refinement of the site occupation factors for the metal atoms showed no significant deviation from unity, with the exception of Nd(2). Refinement of the Nd(2) site occupancy gave a value of 0.966, with a decrease in R factors from R1/wR2 (all data) = 0.0325/0.0679 to R1/wR2 (all data) = 0.0313/0.0648. This could be due to either vacancy or mixing of a lighter atom on this site. These possibilities cannot be distinguished on the basis of the X-ray data alone. For this reason, the occupation factor of Nd2 was set at 1.0 for the final cycles. At convergence, the residual electron density extremes were +1.51/−3.20 $e^-/Å^3$, located in the vicinity of Nd(2).

Similarly for $Pr_{14}Na_3Ru_6O_{36}$, systematic absences in the intensity data indicated the space groups $R3c$ and $R\bar{3}c$, the latter of which was confirmed. $Pr_{14}Na_3Ru_6O_{36}$ is isostructural with $Nd_{14}Na_3Ru_6O_{36}$. Refinement of the structural model obtained from $Nd_{14}Na_3Ru_6O_{36}$ converged rapidly with no unusual atomic behavior. All atoms, including oxygens, were refined with anisotropic displacement parameters. Due to the presence of Os in the reaction mixture, the possibility of Ru/Os mixing in the data crystal was examined by refining the Ru site occupancies. The three independent Ru sites each showed a slight increase above full occupancy, indicating a small amount of Os may be present on those sites. Refinement of each site as a mixture of Ru and Os gave a composition of $Pr_{14}Na_3(Ru_{5.83}Os_{0.17})O_{36}$. Due to the very small Os fraction, occupancies for the three Ru sites were fixed at 100% Ru for the final cycles.

(9) Claridge, J. B.; Layland, R. C.; Henley, W. H.; zur Loye, H.-C. *Chem. Mater.* **1999**, *11*, 1376.
(10) Frenzen, S.; Müller-Buschbaum, H. *Z. Naturforsch., B: Chem. Sci.* **1995**, *50b*, 581.
(11) Reisner, B. A.; Stacy, A. M. *J. Am. Chem. Soc.* **1998**, *120*, 9682.
(12) Smith, M. D.; Stalick, J. K.; zur Loye, H.-C. *Chem. Mater.* **1999**, *11*, 2984.
(13) Stitzer, K. E.; Darriet, J.; zur Loye, H. C. *Curr. Opin. Solid State Mater. Sci.* **2001**, *5*, 535.
(14) Wehrum, G.; Hoppe, R. *Z. Anorg. Allg. Chem.* **1992**, *617*, 45.
(15) Gemmill, W. R.; Smith, M. D.; zur Loye, H.-C. *Inorg. Chem.* **2004**, *43*, 4254.
(16) (a) *SAINT+*, version 6.22; Bruker Analytical X-ray Systems, Inc.: Madison, Wisconsin, 2001. (b) *SMART*, version 5.625; Bruker Analytical X-ray Systems, Inc.: Madison, Wisconsin, 2001. (c) *SADABS*, version 2.05; Bruker Analytical X-ray Systems, Inc.: Madison, Wisconsin, 2001.
(17) Sheldrick, G. M. *SHELXTL*; Bruker Analytical X-ray Systems, Inc.: Madison, Wisconson, 2000.

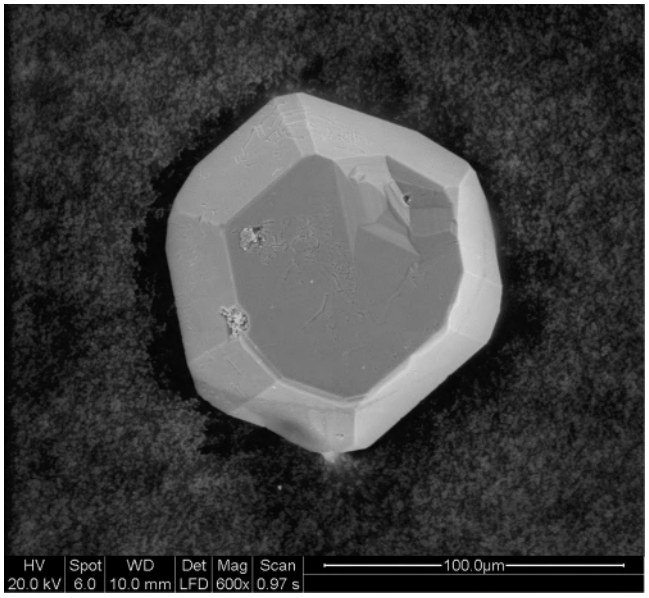

Figure 1. ESEM image of a flux-grown $Pr_{14}Na_3Ru_6O_{36}$ crystal.

Refinement of the Pr occupancies showed no significant deviation from unity occupancy in either case. At convergence, the residual electron density extremes were $+1.66/-4.12$ e$^-$/Å^3, located in the vicinity of Pr(1).

C. Scanning Electron Microscopy. Environmental scanning electron micrographs (ESEM) of several single crystals were obtained using a FEI Quanta 200 ESEM instrument in the low vacuum mode. An ESEM image of $Pr_{14}Na_3Ru_6O_{36}$ is shown in Figure 1. The ESEM also verified the presence of neodymium, sodium, ruthenium, and oxygen for all samples of $Nd_{14}Na_3Ru_6O_{36}$ and praseodymium, sodium, ruthenium, and oxygen for $Pr_{14}Na_3Ru_6O_{36}$. There was a small amount (<2 atom %) of osmium detected in the analysis of the crystals of $Pr_{14}Na_3Ru_6O_{36}$; however, although the crystals were cleaned by sonication, it is difficult to ascertain whether the osmium is just present on the surface of the crystal or actually incorporated into the crystal. Finally, within the detection limits of the instrument, EDS demonstrated the absence of other elements in the crystals.

D. Magnetic Susceptibility. The magnetic susceptibility of title compounds was measured using a Quantum Design MPMS XL SQUID magnetometer. For the magnetic measurements, loose crystals of $Ln_{14}Na_3Ru_6O_{36}$ (Ln = Pr, Nd) were placed into a gelatin capsule, which was placed inside a plastic straw. The samples were measured under both zero-field-cooled (ZFC) and field-cooled (FC) conditions. For all measurements, the total magnetic moment was measured in the temperature range of 2−300 K. Measurements were carried out in applied fields between 500 G and 10 kG. In addition, field sweeps were recorded between +40 and −40 kG at 100 and 2 K. The very small diamagnetic contribution ($\sim 10^{-6}$ emu) of the gelatin capsule containing the sample had a negligible contribution to the overall magnetization, which was dominated by the sample signal.

Results and Discussion

A. Crystal Structure. The title compounds, $Ln_{14}Na_3Ru_6O_{36}$ (Ln = Pr, Nd), crystallize with trigonal (rhombohedral) symmetry in the space group $R\bar{3}c$ with lattice parameters $a = 9.6718(2)$ and $c = 55.4156(18)$ Å for $Nd_{14}Na_3Ru_6O_{36}$ and $a = 9.7380(2)$ and $c = 55.5716(18)$ Å for $Pr_{14}Na_3Ru_6O_{36}$. Crystallographic data and structure refinement information for both compounds are compiled in Table 1, atomic positions and displacement parameters are listed in Table 2, and selected interatomic distances and bond angles for both compounds are collected in Table 3. The structure is composed of two types of slabs that alternate in an AB fashion. These slabs, consisting of three layers each, are propagated via a 3_1 screw axis to yield a unit cell with a 12-layer structure. Each slab is discussed in detail in the following. The complete structure of $Nd_{14}Na_3Ru_6O_{36}$ is shown in Figure 2.

A.1. Slab 1, $Ln(1)_6[Na(2)Ln(3)]_2Na(1)Ru(1)_3O_{18}$. Slab 1 is shown in Figure 3. There are two distinct layers that

Table 1. Crystallographic Data and Structure Refinement of $Ln_{14}Na_3Ru_6O_{36}$ (Ln = Pr, Nd)

empirical formula	$Pr_{14}Na_3Ru_6O_{36}$	$Nd_{14}Na_3Ru_6O_{36}$
formula weight	3224.13 g/mol	3270.75 g/mol
temperature	294(2) K	293(2) K
wavelength	0.71073 Å	0.71073 Å
crystal system	trigonal	trigonal
space group	$R\bar{3}c$	$R\bar{3}c$
unit cell dimensions	$a = 9.7380(2)$ Å $c = 55.5716(18)$ Å	$a = 9.6781(2)$ Å $c = 55.4156(18)$ Å
volume	4563.76 (18) Å^3	4495.1(2) Å^3
Z	6	6
density (calcd)	7.039 Mg/m^3	7.249 Mg/m^3
absorption coefficient	24.974 mm^{-1}	26.850 mm^{-1}
reflns collected	19736	16240
independent reflns	1855 [R(int) = 0.0751]	1878 [R(int) = 0. 0394]
abs correction	semiempirical from equivalents	semiempirical from equivalents
data/restraints/parameters	1855/0/91	1878/0/91
GOF on F^2	1.087	1.165
final R indices [$I > 2\sigma(I)$]	R1 = 0.0368, wR2 = 0.0727	R1 = 0.0320, wR2 = 0.0677
R indices (all data)	R1 = 0.0417, wR2 = 0.0744	R1 = 0.0325, wR2 = 0.0679
largest diff. peak and hole	1.663 and −4.122 e Å^{-3}	1.506 and −3.197 e Å^{-3}

Table 2. Atomic Coordinates and Equivalent Isotropic Displacement Parameters for $Ln_{14}Na_3Ru_6O_{36}$ (Ln = Pr, Nd)

$Pr_{14}Na_3Ru_6O_{36}$	x	y	z	U(eq)
Pr(1)	0.0047(1)	0.2885(1)	0.2166(1)	0.005(1)
Pr(2)	0.0289(1)	0.3429(1)	0.1478(1)	0.006(1)
Pr(3)	0	0	0.1080(1)	0.006(1)
Ru(1)	−0.0005(1)	0.3333	0.0833	0.002(1)
Ru(2)	0	0	0	0.003(1)
Ru(3)	0	0	0.1625(1)	0.003(1)
Na(1)	0	0	0.2500	0.009(2)
Na(2)	0	0	0.0534(1)	0.013(1)
O(1)	0.1976(7)	0.1916(7)	0.2240(1)	0.007(1)
O(2)	0.1954(7)	0.1296(7)	0.1413(1)	0.009(1)
O(3)	0.0655(7)	0.1983(7)	0.1796(1)	0.008(1)
O(4)	0.2338(7)	0.1349(7)	0.0817(1)	0.007(1)
O(5)	0.1443(7)	0.3554(7)	0.0578(1)	0.007(1)
O(6)	0.1660(7)	0.1703(7)	0.0206(1)	0.010(1)
$Nd_{14}Na_3Ru_6O_{36}$	x	y	z	U(eq)
Nd(1)	0.0038(1)	0.2882(1)	0.2167(1)	0.006(1)
Nd(2)	0.0307(1)	0.3441(1)	0.1476(1)	0.008(1)
Nd(3)	0	0	0.1077(1)	0.006(1)
Ru(1)	−0.0005(1)	0.3333	0.0833	0.003(1)
Ru(2)	0	0	0	0.003(1)
Ru(3)	0	0	0.1626(1)	0.004(1)
Na(1)	0	0	0.2500	0.010(1)
Na(2)	0	0	0.0535(1)	0.012(1)
O(1)	0.1965(6)	0.1912(6)	0.2240(1)	0.007(1)
O(2)	0.1940(6)	0.1273(6)	0.1411(1)	0.008(1)
O(3)	0.0658(6)	0.1967(6)	0.1796(1)	0.007(1)
O(4)	0.2334(6)	0.1353(6)	0.0819(1)	0.007(1)
O(5)	0.1449(6)	0.3553(6)	0.0578(1)	0.007(1)
O(6)	0.1682(6)	0.1699(6)	0.0207(1)	0.009(1)

Table 3. Selected Interatomic Distances (Å) for $Ln_{14}Na_3Ru_6O_{36}$ (Ln = Pr, Nd)

	$Pr_{14}Na_3Ru_6O_{36}$	$Nd_{14}Na_3Ru_6O_{36}$
Ln(1)−O	2.522(6)	2.505(5)
	2.476(6)	2.460(5)
	2.368(6)	2.362(5)
	2.425(6)	2.428(5)
	2.633(6)	2.608(5)
	2.449(6)	2.434(5)
	2.457(6)	2.446(5)
	2.475(6)	2.456(5)
Ln(2)−O	2.667(6)	2.656(5)
	2.373(6)	2.359(5)
	2.392(6)	2.402(5)
	2.452(6)	2.444(5)
	2.426(6)	2.406(5)
	2.533(6)	2.524(5)
	2.618(6)	2.608(5)
	2.780(6)	2.733(5)
Ln(3)−O(4)	2.459(6) × 3	2.431(5) × 3
Ln(3)−O(2)	2.498(6) × 3	2.482(5) × 3
Ln(3)−O(5)	2.646(6) × 3	2.630(5) × 3
Ru(1)−O(5)	1.936(5) × 2	1.932(5) × 2
Ru(1)−O(1)	1.975(6) × 2	1.973(5) × 2
Ru(1)−O(4)	1.986(6) × 2	1.981(5) × 2
Ru(2)−O(6)	1.997(6) × 6	1.996(5) × 6
Ru(3)−O(3)	1.950(6) × 3	1.925(5) × 3
Ru(3)−O(2)	2.050(6) × 3	2.036(5) × 3
Na(1)−O(1)	2.383(6) × 6	2.368(5) × 6
Na(2)−O(6)	2.451(8) × 3	2.448(6) × 3
Na(2)−O(4)	2.529(7) × 3	2.515(6) × 3

compose this slab. The first has the composition $Ln(1)_3[Na(2)Ln(3)]O_6$ and the second $Na(1)Ru(1)_3O_6$. They are arranged A−B−A′, where A′ represents A propogated through the inversion center, and the layers are compositionally equivalent. Na(1) is located in trigonal prismatic coordination, and the Na(1)−O bond lengths are 2.383(6) and 2.368(5) Å for $Pr_{14}Na_3Ru_6O_{36}$ and $Nd_{14}Na_3Ru_6O_{36}$, respectively. Similarly, Na(2) exists in trigonal prismatic coordination, albeit distorted, and the Na(2)−O bond lengths are 2.451(8) and 2.529(7) Å for $Pr_{14}Na_3Ru_6O_{36}$ and 2.448(6) and 2.515(6) Å for $Nd_{14}Na_3Ru_6O_{36}$, which are considerably longer than the Na(1)−O bond lengths in the $Na(1)O_6$ trigonal prism. Both sets of Na−O bond lengths are acceptable for NaO_6 polyhedra.[18−21] Ru(1) exists in octahedral coordination and shares an edge with a $Na(1)O_6$ trigonal prism. The Ru(1)−O bond lengths vary between 1.936(5) and 1.986(6) Å for $Pr_{14}Na_3Ru_6O_{36}$ and 1.932(5) and 1.981(5) Å for $Nd_{14}Na_3Ru_6O_{36}$, consistent with the bond lengths in other RuO_6 octahedra.[1,15] This structural feature, the $Na(1)O_6-[Ru(1)O_6]_3$ unit, is reminiscent of the hexagonal iridates exemplified by $Ca_{5-x}Ir_3O_{12}$[22,23] and most closely resembles those found in $LnNaIrO_4$ (Ln = Gd−Er, Y).[24] Na(2) and Nd(3) are effectively disordered on the equivalent site (Na) in $LnNaIrO_4$.

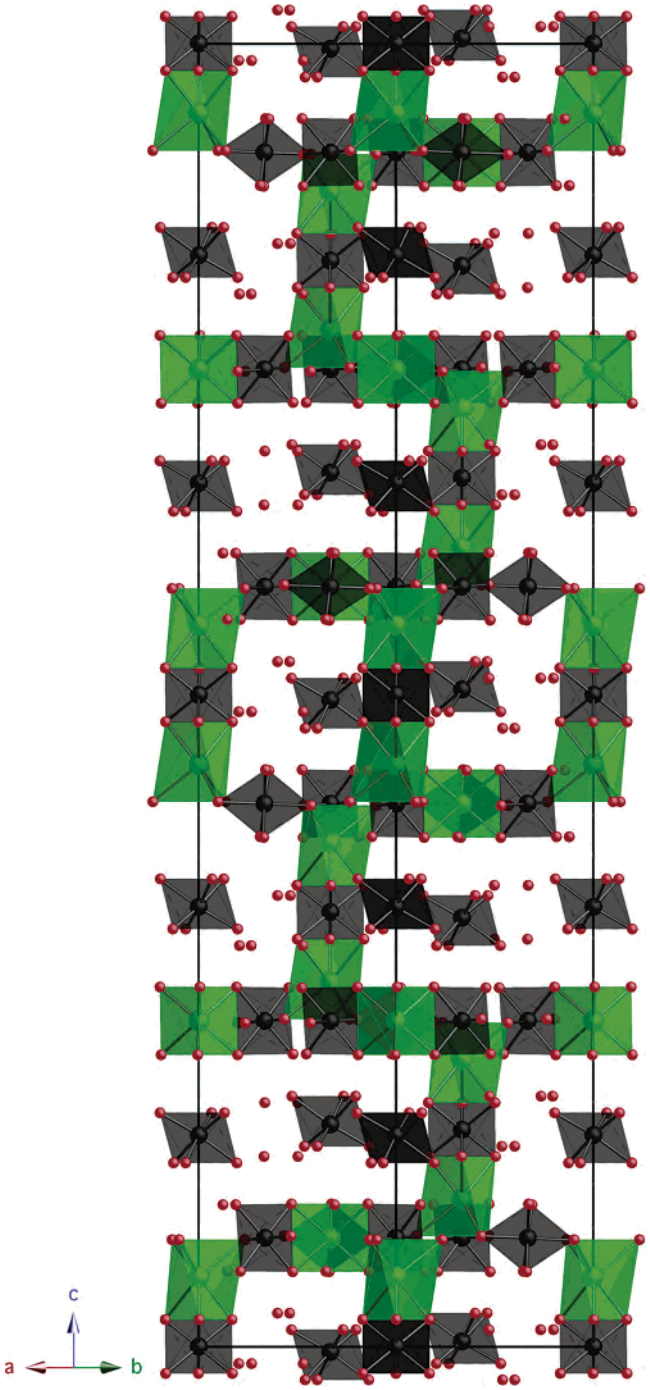

Figure 2. The structure of $Nd_{14}Na_3Ru_6O_{36}$. NaO_6 polyhedra are shown in green, RuO_6 octahedra are shown in black, O atoms are in red, and the Nd^{3+} atoms have been omitted for clarity.

A.2. Slab 2, $Ln(2)_6Ru(2)Ru(3)_2O_{18}$. Slab 2 is shown in Figure 4. As in the first slab, there are two layers that compose slab 2. The first has the composition $Ln(2)_3O_9$ and the second $Ru(2)Ru(3)_2$; the two layers alternate in an A−B−**A′** fashion, where A′ represents A propagated through the inversion center. The $Ru(2)O_6$ octahedra lie in the middle of two $Na(2)O_6$ trigonal prisms (Figure 2) in a face-sharing arrangement of polyhedral columns which resemble those

(18) Battle, P. D.; Hartwell, S. J.; Moore, C. A. *Inorg. Chem.* **2001**, *40*, 1716.
(19) Claridge, J. B.; Layland, R. C.; Adams, R. D.; zur Loye, H.-C. *Z. Anorg. Allg. Chem.* **1997**, *623*, 1131.
(20) Davis, M. J.; Smith, M. D.; zur Loye, H.-C. *Inorg. Chem.* **2003**, *42*, 6980.
(21) Frenzen, S.; Muller-Buschbaum, H. *Z. Naturforsch., B: Chem. Sci.* **1995**, *50b*, 581.
(22) Dijksma, F. J. J.; Vente, J. F.; Frikkee, E.; Ijdo, D. J. W. *Mater. Res. Bull.* **1993**, *28*, 1145.
(23) Wakeshima, M.; Taira, N.; Hinatsu, Y.; Ishii, Y. *Solid State Commun.* **2003**, *125*, 311.
(24) Mugavero, S. J. I.; Smith, M. D.; zur Loye, H.-C. *Solid State Sci.* **2006**, Submitted.

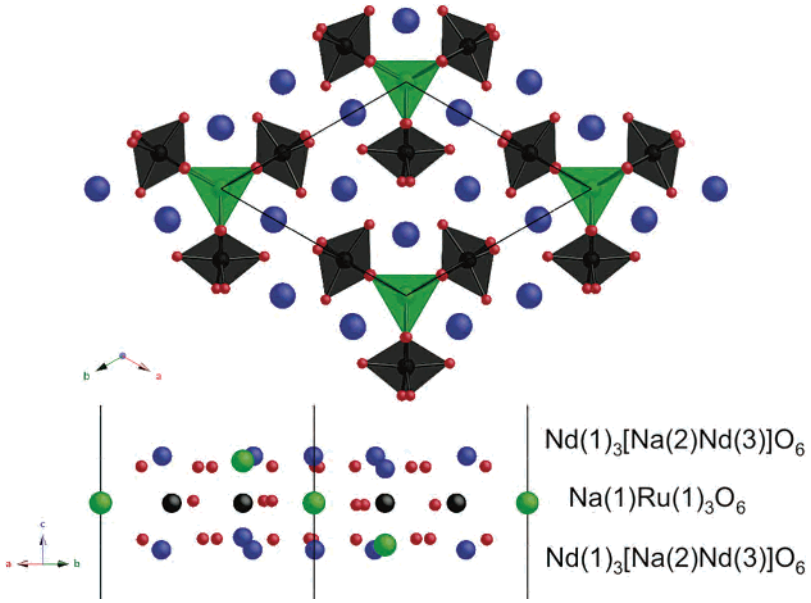

Figure 3. Slab 1. The layers that compose slab 1 are shown down [110] (bottom). Atoms are represented in green (Na), blue (Nd), black (Ru), and red (O). On the top is a polyhedral representation as viewed down *c* and shows the $NaO_6-[RuO_6]_3$ units typically found in hexagonal iridates.[22−24]

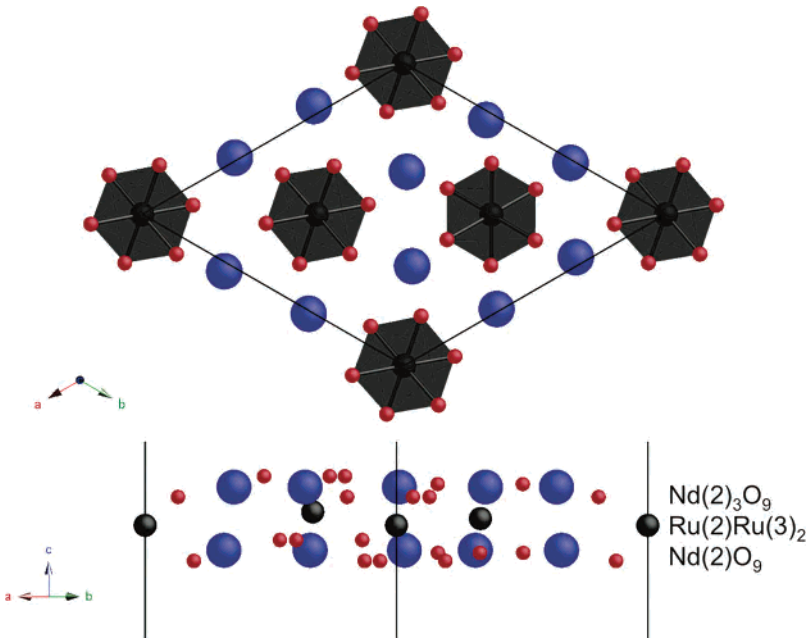

Figure 4. Slab 2. The layers that compose slab 2 are shown down [110] (bottom). Atoms are represented in blue (Nd), black (Ru), and red (O). On the top is a polyhedral representation as viewed down *c* showing the arrangement of RuO_6 octahedra. The RuO_6 octahedra on the cell edges are involved in the $NaO_6-RuO_6-NaO_6$ polyhedral connectivity commonly observed in 2*H*-related perovskites.[13]

in 2*H*-related perovskites.[13] The Ru(2)−O bond lengths are 1.997(6) and 1.996(5) Å for $Ln_{14}Na_3Ru_6O_{36}$ (Ln = Pr, Nd), respectively, which are considerably longer than Ru^{5+}−O bond lengths (∼1.96 Å) found in the A_3NaRuO_6 (A = Ca, Sr) compounds, suggesting that the valence is somewhere in between Ru^{4+} and Ru^{5+}; however, an example of $Ru^{4+}O_6$ octahedra involved in a similar polyhedral arrangement is not known from the literature. The $Ru(3)O_6$ octahedra are isolated and are not involved in the NaO_6/RuO_6 polyhedral connectivity. There are three short and three long Ru(3)−O bond lengths, 1.950(6) and 2.050(6) Å and 1.925(5) and 2.036(5) Å for $Pr_{14}Na_3Ru_6O_{36}$ and $Nd_{14}Na_3Ru_6O_{36}$, respectively. Ln(2) exists in a bicapped trigonal prismatic coordination environment and is involved in the connectivity of slab 2 and slab 1, specifically the $Ru(3)O_6$ (slab 2) octahedra and the $Ru(1)O_6$ (slab 1) octahedra.

The structure of $Ln_{14}Na_3Ru_6O_{36}$ (Ln = Pr, Nd) is very similar to that of $La_7Ru_3O_{18}$.[6] All three compounds share virtually the same arrangement of lanthanide, ruthenium, and oxygen atoms. The difference is that, in the title compounds, sodium is present, occupying coordination sites that are vacant in the structure of $La_7Ru_3O_{18}$. In the title compounds, Na(1) lies in the center of the three $Ru(1)O_6$ octahedra in trigonal prismatic coordination, sharing an edge with each of the aforementioned octahedra. Na(2) lies in between Ru(2) and Ln(3), also in trigonal prismatic coordination,

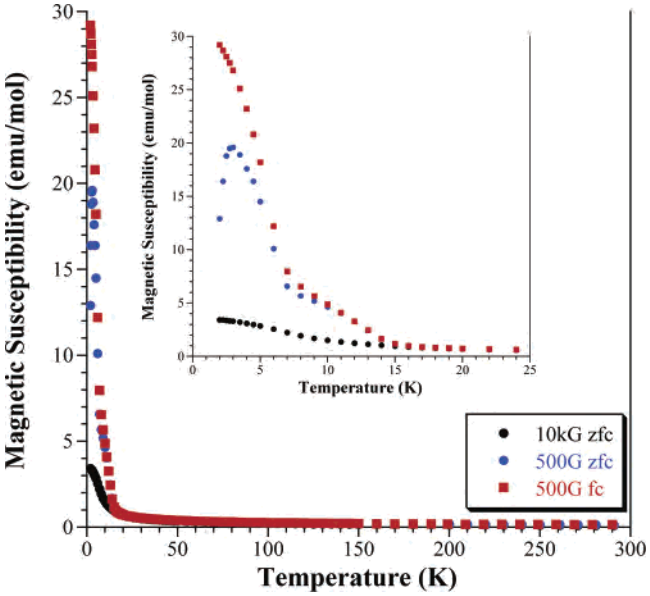

Figure 5. Temperature dependence of the susceptibility of $Nd_{14}Na_3Ru_6O_{36}$ carried out in applied fields of 0.5 and 10 kG.

Table 4. Bond Valence Values (BVS) Calculated Utilizing SPuDS[26] for $Pr_{14}Na_3Ru_6O_{36}$ and $Nd_{14}Na_3Ru_6O_{36}$

$Pr_{14}Na_3Ru_6O_{36}$	BVS	$Nd_{14}Na_3Ru_6O_{36}$	BVS
Pr(1)	3.271	Nd(1)	3.092
Pr(2)	2.953	Nd(2)	2.783
Pr(3)	3.154	Nd(3)	3.052
Ru(1)	5.033	Ru(1)	5.083
Ru(2)	3.862	Ru(2)	3.873
Ru(3)	3.866	Ru(3)	4.084
Na(1)	1.251	Na(1)	1.303
Na(2)	0.942	Na(2)	0.963

sharing its vertical faces with those of the $Ln(3)O_9$ and $Ru(2)O_6$ polyhedra. In contrast, these sites are vacant in $La_7Ru_3O_{18}$. From this analysis, the title compounds could be referred to as sodium-stuffed analogues of $La_7Ru_3O_{18}$. This "stuffing" of sodium effectively lowers the average oxidation state of ruthenium from +5 in $La_7Ru_3O_{18}$ to +4.5 in $Ln_{14}Na_3Ru_6O_{36}$ (Ln = Pr, Nd).

The average oxidation state of +4.5 for ruthenium in $Ln_{14}Na_3Ru_6O_{36}$ (Ln = Pr, Nd) suggests that both ruthenium +4 and ruthenium +5 are present. To differentiate between a random +4/+5 distribution and a charge-ordered arrangement of ruthenium in the structure,[4] we have carried out a bond valence analysis.[25,26] The results shown in Table 4 suggest that Ru(1) is present in the +5 oxidation state, while Ru(2) and Ru(3) are present in the +4 oxidation state. The assignments of the ruthenium oxidation states, coupled with the site multiplicities, 18, 6, and 12, for Ru(1), Ru(2), and Ru(3), respectively, result in the correct average oxidation state of +4.5.

B. Magnetism. The temperature dependence of the magnetic susceptibility for $Nd_{14}Na_3Ru_6O_{36}$, measured in applied fields of 0.5 and 10 kG, is shown in Figure 5. The most notable feature of the temperature sweeps is that, at fields below 1 kG, the zero-field-cooled (ZFC) and field-cooled (FC) data do not overlay below about 10 K (Figure 5, inset). Figure 6 shows the field dependence of the magnetization for $Nd_{14}Na_3Ru_6O_{36}$. At 100 K, no field dependence is observed, while at 2 K, a field dependence is observed with an unsaturated moment of about 11 μ_B at 40 kG. This behavior is consistent with either a canted antiferromagnetic or a ferrimagnetic state. A χ^*T versus T plot is shown in Figure 7, where the magnetic moment can be seen to decrease toward lower temperature, consistent with antiferromagnetic interactions, followed by a rapid increase in the magnetic moment near 10 K. Fitting the high-temperature susceptibility data ($100 \leq T \leq 300$) of $Nd_{14}Na_3Ru_6O_{36}$ to the Curie−Weiss Law yields an effective moment of 17.1 μ_B, with $\theta = -58.2$ K. The theoretical moment for $Nd_{14}Na_3Ru_6O_{36}$ is 15.9 μ_B,[27] lower than the experimentally determined value; the reason for this is unclear at present.

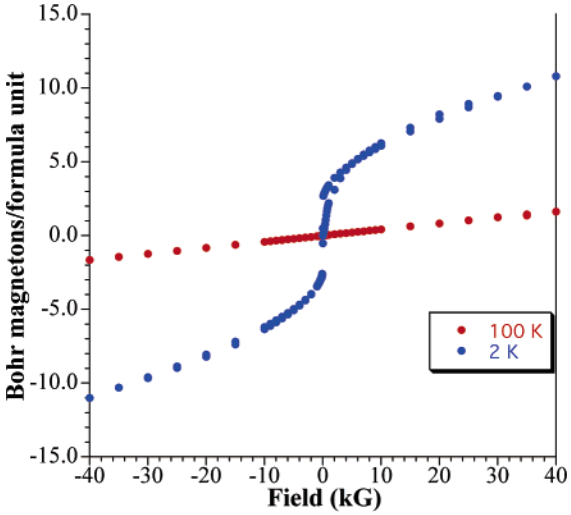

Figure 6. Field dependence of the magnetization of $Nd_{14}Na_3Ru_6O_{36}$ measured at 100 and 2 K.

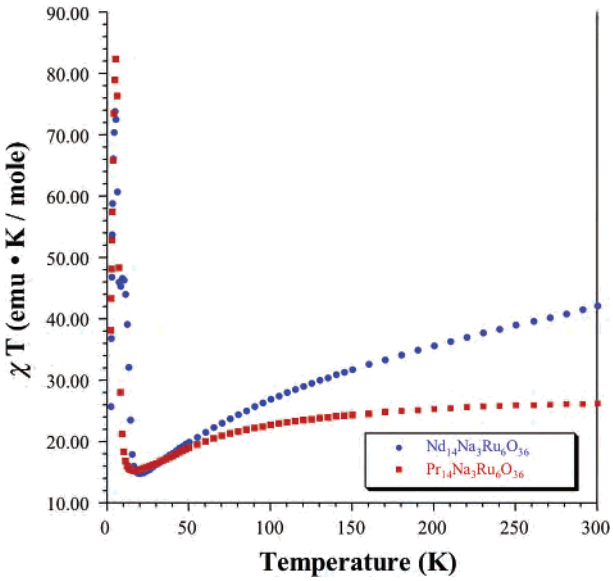

Figure 7. χ^*T versus T plot for $Nd_{14}Na_3Ru_6O_{36}$ and $Pr_{14}Na_3Ru_6O_{36}$.

(25) Brese, N. E.; O'Keeffe, M. O. *Acta Crystallogr., Sect. B* **1991**, *47*, 192.
(26) Lufaso, M. W.; Woodward, P. M. *Acta Crystallogr., Sect. B* **2001**, *57*, 725.

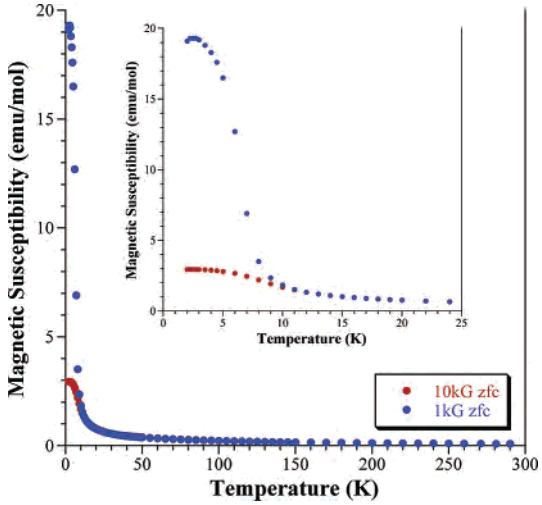

Figure 8. Temperature dependence of the susceptibility of $Pr_{14}Na_3Ru_6O_{36}$ carried out in applied fields of 1 and 10 kG.

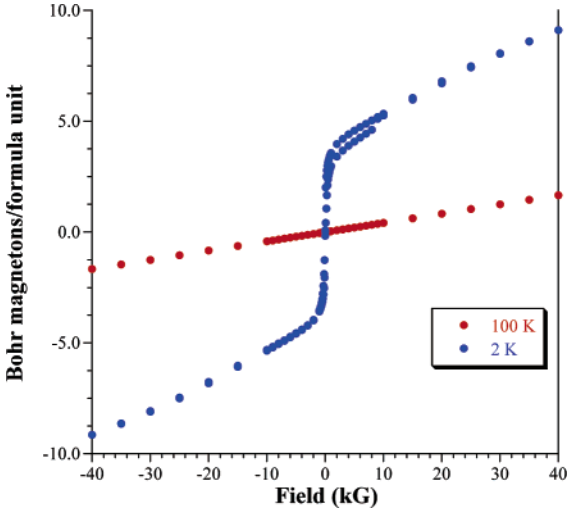

Figure 9. Field dependence of the magnetization of $Pr_{14}Na_3Ru_6O_{36}$ measured at 100 and 2 K.

The temperature dependence of the magnetic susceptibility for $Pr_{14}Na_3Ru_6O_{36}$, measured in applied fields of 1 and 10 kG, is shown in Figure 8. At about 8 K, the susceptibility increases in a ferromagnetic-like manner, most noticeably in an applied field of 1 kG. Figure 9 shows the field dependence of the magnetization for $Pr_{14}Na_3Ru_6O_{36}$. At 100 K, no field dependence is observed, but at 2 K, a field dependence is observed with an unsaturated moment of about 9 μ_B at 40 kG. As in $Nd_{14}Na_3Ru_6O_{36}$, the magnetic behavior of $Pr_{14}Na_3Ru_6O_{36}$ is consistent with either a canted antiferromagnetic or a ferrimagnetic state. The χ^*T versus T plot shown in Figure 7 also shows a decrease in the magnetic moment toward lower temperature, consistent with antiferromagnetic interactions, followed by a rapid increase in the moment near 10 K. Fitting the high-temperature susceptibility data ($100 \leq T \leq 300$) of $Pr_{14}Na_3Ru_6O_{36}$ to the Curie−Weiss Law yields an effective moment of 15.0 μ_B, with $\theta = -21.5$ K. The theoretical moment for $Pr_{14}Na_3Ru_6O_{36}$ is 15.7 μ_B,[28] which is in good agreement with the experimentally determined moment. However, due to the possibility of the presence of a slight amount of osmium substitution in $Pr_{14}Na_3Ru_6O_{36}$, these values may not reflect the moment for a stoichiometrically pure ruthenate.

(27) The theoretical magnetic moment for $Nd_{14}Na_3Ru_6O_{36}$ was calculated by combining the spin-only approximation for Ru^{4+} and Ru^{5+} and the Russell−Saunders coupling for Nd^{3+} in the following equation: $\mu = \sqrt{((14 \times Nd(III)^2) + (3 \times Ru(IV)^2) + (3 \times Ru(V)^2))}$; $\mu = \sqrt{((14 \times 3.62^2) + (3 \times 2.83^2) + (3 \times 3.87^2))}$; $\mu = 15.9$ μ_B.

(28) The theoretical magnetic moment for $Pr_{14}Na_3Ru_6O_{36}$ was calculated by combining the spin-only approximation for Ru^{4+} and Ru^{5+} and the Russell−Saunders coupling for Pr^{3+} in the following equation: $\mu = \sqrt{((14 \times Pr(III)^2) + (3 \times Ru(IV)^2) + (3 \times Ru(V)^2))}$; $\mu = \sqrt{((14 \times 3.58^2) + (3 \times 2.83^2) + (3 \times 3.87^2))}$; $\mu = 15.7$ μ_B.

Conclusions

The two new compounds, $Ln_{14}Na_3Ru_6O_{36}$ (Ln = Pr, Nd), were grown as single crystals out of molten sodium hydroxide. The growth of these oxides from molten sodium hydroxide fluxes further establishes these melts as a successful solvent system for both the preparation of new and unique oxide structures and compounds containing a lanthanide and a platinum group metal. Structurally related to $La_7Ru_3O_{18}$, $Ln_{14}Na_3Ru_6O_{36}$ (Ln = Pr, Nd) can be considered a sodium-stuffed modification of the former. These structures represent a unique example containing structural units similar to the hexagonal iridates, $Ca_{5-x}Ir_3O_{12}$ and $LnNaIrO_4$, and 2*H*-perovskites. Both compounds show magnetic behavior consistent with canted antiferromagnetism.

Acknowledgment. Financial support for this research was provided by the Department of Energy through Grant DE-FG02-04ER46122 and the National Science Foundation through Grant DMR:0450103.

Supporting Information Available: CIF files for $Ln_{14}Na_3Ru_6O_{36}$ (Ln = Pr, Nd). This material is available free of charge via the Internet at http://pubs.acs.org.

IC0617083